EXCITATION OF DIELECTRONIC SATELLITES OF RESONANCE LINES OF Cd^+ IONS IN ELECTRON-ION COLLISIONS

A.N. GOMONAI, A.I. IMRE

Institute of Electron Physics, Nat. Acad. Sci. of Ukraine
(21, Universytets'ka Str., Uzhgorod 88017; e-mail: dep@mail.uzhgorod.ua),

UDC 539.186/.188

Identification of subthreshold structures in the experimentally studied energy dependences of effective electron excitation cross sections for $\lambda = 226.5$ and 214.4 nm resonance lines of Cd^+ ions is suggested. The experiment was performed by spectroscopic method using the monoenergetic electron and ionic beams crossed at 90° angle. It has been found that the subthreshold features are due to the resonant capture of an incident electron by an ion, excitation of the "electron + Cd^+ ion" system into the $4d^{10}5p(^2P_{1/2,3/2})nl$ autoionizing states (AIS), and their decay to the excited $4d^{10}5snl$ states of an Cd atom, i.e. the features are the dielectronic satellites of resonance lines. Absolute values of the excitation cross sections for the dielectronic satellites are $(0.2 \div 1) \cdot 10^{-16}$ cm^2 and are of the same order of magnitude as the effective excitation cross sections for resonance lines of Cd^+ ion. It has been shown that the considerable rise in the probability of radiative decay of the autoionizing $4d^{10}5p(^2P_{1/2,3/2})nl$ states of Cd atom is related to a strong configuration mixing of the above states.

Introduction

The presence of the long-range Coulomb field of an ion in electron-ion collisions leads to the resonance excitation of an ion if the electron energy is less than the threshold one. This is accompanied by the capture of an incident electron by the field of an excited ion and by the excitation of the "electron + Cd^+ ion" system in an autoionizing state (AIS) which has two decay channels: electron and radiative ones. The electron decay channel of AIS reveals itself as resonances in the cross sections of electron-ion elastic scattering in the energy region below the thresholds of new channels and as resonances in the ion excitation cross sections above the thresholds. The radiative decay channel of AIS causes the dielectronic recombination (DR) of an ion.

For the first time, the mechanism of DR was described by H. Massey and D. Bates in [1]. But only beginning from work [2], a considerable (sometimes decisive) role of this process in both the ionization equilibrium formation and the evolution of plasma (in particular, the solar corona plasma) was comprehended. In [3], three most significant manifestations of DR were discussed: a) the DR proper as the process that is decisive for the ionization equilibrium of plasma in many cases; b) satellites of resonant and other lines of an ion that appear in radiative transitions from AIS, the so-called dielectronic satellites (DS) that occur in the spectra of plasma during its recombination (e.g., in the spectra of solar flares, laser plasma, plasma of tokamaks, etc.); c) additional excitation of ionic levels under the realization of the electron decay channel of AIS (additional satellites) that plays no considerable role in the total balance of DR.

In the first two cases, the photon emission occurs in the transition of an "internal" AIS electron and the state of an external electron is not changed. A radiative transition of the external electron yields additional satellites.

Dielectronic satellites (as usual, those of resonance lines) have wavelengths close to those of the relevant spectral line of an ion and are very convenient to make diagnostics of laboratory and astrophysical plasmas, because the ratio of the intensities of satellites and resonance lines depends considerably on temperature.

The very first of our experimental studies of the near-threshold excitation of complicated multielecton atomic systems such as Tl^+[4] and Zn^+ [5] ions under their collisions with monoenergetic electrons showed that values of the effective excitation cross-sections of the resonance lines of these ions and the relevant DS are of the same order of magnitude. This provided evidence for a large probability of the radiative decay channel for atomic AIS formed in the collisions of electrons with Tl^+ and Zn^+ ions, which was explained by a strong influence of relativistic effects and a significant configuration mixing of AIS on the mechanisms of these processes. Therefore, the main attention was given to studying the electron excitation of the DS of Cd^+ ions,

$$e + Cd^+(4d^{10}5s)^2S_{1/2} \to Cd^{**}[4d^{10}5p(^2P_{1/2,3/2})nl] \to$$

$$\to Cd^*(4d^{10}5snl) + h\nu_n, \qquad (1)$$

for which the influence of relativistic and correlation effects on the mechanisms of direct and resonant excitations is stronger as compared with that for Zn^+ ions. We performed the precise investigations of the near-threshold areas of the energy-dependent effective excitation cross-sections of resonance lines of Cd^+ ion by monoenergetic ($\Delta E_{1/2} \approx 0.35$ eV) electrons [6] at energies less than the excitation thresholds for resonance levels and discovered a number of subthreshold maxima.

In the present paper, we clarify the explanation proposed by us as for the nature of the discovered subthreshold maxima of resonance lines of Cd^+ ion as the DS of these lines and give their identification.

1. Experimental Setup and Method

The experiment was performed by a spectroscopic method with electron and Cd^+ ion beams that intersected at 90° angle. The main units of the experimental setup are schematically presented in Fig. 1.

The source of Cd^+ ions operated in the mode of low-voltage arc discharge and included container *1* with a working substance *2*, ionization chamber *3* with a directly heated cathode *4* manufactured from a thoriated tungsten wire 0.2 mm in diameter in the form of a spiral (with an internal diameter of 1 mm, 3—4 turns), and a system of their heating. The temperature mode of operation of the source was set by heating the container and the ionization chamber with the use of a highly stabilized power supply. With the purpose to reach a necessary concentration of atoms and to prevent the deposition of the working substance on the chamber walls, the temperature of the ionization chamber was

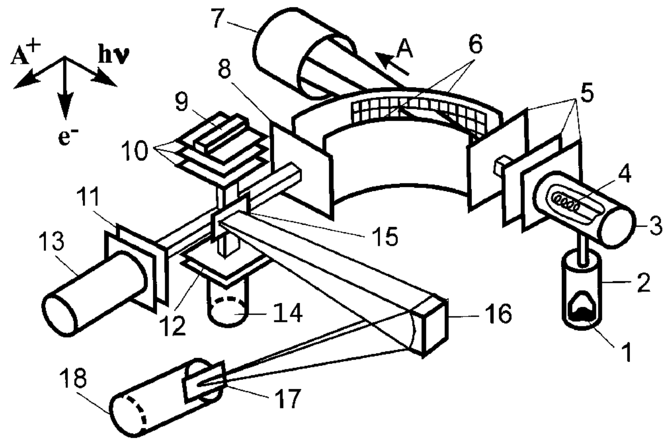

Fig. 1. Scheme of the main units of the experimental setup: *1* — ampoule with working substance, *2* — container, *3* — ionization chamber, *4* — cathode of the ion source, *5* — ion-optical system, *6* — plates of the electrostatic 90°-capacitor, *7* — trap for atoms, *8* — forming slit, *9* — cathode of the electron gun, *10* — electron-optical system, *11* ,*12* — electrodes for capture of secondary electrons, *13* — collector of ions, *14* — collector of electrons, *15* — input slit of the monochromator, *16* — diffraction grating, *17* — output slit, *18* — detector of emission

chosen to be somewhat greater than that of the container. The pressure of saturated vapours of Cd atoms in the discharge chamber was $\sim 10^{-3}$ Torr.

The withdrawal of ions from the source, shaping and focusing in a beam, and their acceleration up to a necessary energy was realized with the system of electrostatic lenses *5* which were manufactured in the form of truncated cones with the purpose to improve conditions for the derivation of an ion beam. Voltage for the acceleration of ions was supplied on the discharge chamber of the source relative to ground. Then ions were turned by 90° with the electrostatic capacitor *16*. In the vertical plane, the ion beam was focused by two parallel insulated metallic plates fixed between the capacitor plates, on which we supplied a relevant negative potential relative to ground. Neutral atoms of the working substance effused from the source, passed the external plate of the capacitor made of a tungsten grid with transparency of 90%, and entered into a special trap *7* cooled with liquid nitrogen. The initial grounded slit *8*, which was positioned behind the capacitor, formed an ion beam uniform in density with a cross section of 2.5×2.5 mm^2. The beam passed the equipotential region of collisions and got into an ion collector, a deep Faraday cup *13.* To prevent the entry of scattered and reflected electrons into the collector and to entrap secondary electrons produced by ion impact on the internal surface of the collector, we positioned diaphragm *11* in front of it. The diaphragm was supplied with a negative potential relative to ground.

Because Cd^+ ions have the long-lived $4d^9 5s^2 \, {}^2D_{5/2,3/2}$ states with lifetimes of 830 and 300 ns, the ions present in the source were efficiently excited to these states at discharge voltages $U_r > 20$ V. Having no time to decay on the way to the region of collisions, the excited ions made a considerable contribution to the radiative background. Therefore, to minimize the possibility of excitation of ions to the long-lived states, we decreased the discharge voltage up to $U_r \leq 12$ V, i.e. up to a value less than the excitation threshold (17.6 eV) from the ground $4d^{10} 5s^2 \, {}^1S_0$-state of Cd atom to the $4d^9 5s^2 \, {}^2D_{5/2}$-state of Cd^+ ion. Such an operation mode and a number of technical improvements of the construction of the ion source allowed us to form a stable 600-eV beam of Cd^+ ions mainly in the ground state with a current of $(5 \div 7) \cdot 10^{-7}$ A.

The electron beam was formed with the use of a low-energy three-anode gun that operated in the mode of longitudinal compression: electrons emitted from the heated surface of an oxide cathode were firstly accelerated in the "cathode — second anode" gap and then decelerated in the "second anode — third anode" gap. The focusing of electrons was realized by the choice of a positive potential on the first anode. To create the equipotential region of collisions, we grounded the third anode and supplied a voltage for the acceleration of electrons on cathode *9* relative to ground. The rectangular slits on three anodes *10* formed a ribbon beam of electrons with a cross section of 1×8 mm^2 in the range (4÷10) eV with a current of $(5 \div 10) \cdot 10^{-5}$ A. Having passed the equipotential region of collisions, electrons got into electron collector *14* which included the external Faraday cup *12* with the inlet of 3×12 mm^2 closed by a tungsten grid with transparency of 90% and the internal collector manufactured in the form of a parallelepiped which were positioned on the axis. To entrap secondary and scattered electrons, we supplied a negative potential relative to ground on the external Faraday cup with a value being less than the energy of electrons of the beam. The cross section of the internal collector was 2×10 mm^2, which was somewhat greater than that of the electron beam. This allowed us to control the beam geometry in the whole energy range of electrons, by keeping the constancy of the ratio of currents on each collector.

We carried out the pilot experiments for the choice of optimum operating mode of the electron gun which showed that its best parameters (the width on a half height of the energy distribution function of electrons, $\Delta E_{1/2}$, and the energy at which the voltage-current characteristic attains the saturation level) are reached if the gun is adjusted on the accelerating potential ≤ 5 V. In this case, the monoenergeticity of the electron beam was $\Delta E_{1/2} \approx 0.35$ eV in the energy region under study, (4÷7) eV.

The electron and ion beams intersected in the collision region at 90° angle. The emission was observed normally to the intersection plane and was spectrally separated with a vacuum 70°-monochromator VM-70 (15—17, see Fig. 1) manufactured by the Seya — Namioka scheme at our laboratory with the concave toroidal diffraction grating of 1200 line/mm (16) that was covered with Al and worked mainly in the wavelength region of (200÷300) nm. The mean inverse linear dispersion of a monochromator VM-70 was 1.7 nm/mm. Photons were detected with a photoelectric multiplier FEU-142 which was cooled by liquid nitrogen with the purpose to decrease the dark background up to 0.2 pulse/sec. To provide the necessary differentiation of vacuum between the region of collisions ($P \sim 10^{-8}$ Torr) and a monochromator VM-70 ($P \sim 2 \cdot 10^{-7}$ Torr) which was created by oil-free evacuation, the emission passed from the region of collisions through a long cone-like channel.

One of the peculiarities of the experimental study of processes occurring in electron-ion collisions is the need to use very low intensities ($N_{e,i} \leq 10^8$ cm^{-3}) of beams to decrease a strong influence of their spatial charges. This circumstance yields that the signal characterizing the process under study is very slight. In addition, it is detected against both the dominant background from various accompanying processes (collisions of electrons and ions with atoms and molecules of the residual gas) and the background of the emission detector. Because the backgrounds from collisions correlate with the electron or ion beam, they can be separated into two components: Φ_e – background from the electron beam and Φ_i – background from the ion beam. Depending on specific conditions of the experiment, each of the backgrounds can considerably exceed the other or their contributions can be of the same order. We separated a valid signal from the background by using the modulation of both the electron and ion beams, as well as the registration of emission in the counting mode with four counting channels. The general idea of this method is illustrated by the scheme displayed in Fig. 2.

Both the beams of charged particles were modulated by rectangular voltage pulses. In this case, the top and the bottom of a pulse correspond, respectively, to the presence of a given beam and its absence in the region of collisions in a given half of the modulation period. Because the modulating pulses are shifted one relative to another by a quarter of the modulation period, the beams are present in the region of collisions only in a certain sequence that is cyclically repeated. Every quarter of the modulation period corresponds to one of the four counting channels, the pulses from which go into the separate pulse counters. In this case, each counter accumulates pulses during only that quarter of the modulation period which corresponds to this counter. Thus, in the every quarter of the modulation period, we detected the emission arising from different processes in the region of collision by the following scheme:

I quarter: beams are absent; the dark background of the detector Φ_d is registered,

II quarter: there is the electron beam in the collision region; we register Φ_d and the background from collisions of the electron beam with particles of the residual gas and atoms of the working substance, Φ_e: $(\Phi_d + \Phi_e)$,

III quarter: there are the electron and ion beams simultaneously; we register Φ_d, the backgrounds from collisions of the electron and ion beams with particles of the residual gas and working substance, Φ_e and Φ_i, and a valid signal C: $(\Phi_d + \Phi_e + \Phi_i + C)$,

IV quarter: there is the ion beam; we register $(\Phi_d + \Phi_i)$.

Thus, the registration of pulses from the emission detector was implemented by using four controlled counting channels. If we subtract the sum of pulses accumulated during the II and IV quarters, $(2\Phi_d + \Phi_e + \Phi_i)$, from that accumulated during I and III ones, $(2\Phi_d + \Phi_e + \Phi_i + C)$, we get the valid signal C that is defined by the studied process occurring in the collision of electrons with ions.

In our experiments, the signal from the electron excitation of satellites of the resonance lines of Cd^+ ion was 1÷2 pulse/s at the maximum of the excitation functions (EF), and the signal-to-noise ratio was 1/20.

As an important experimental problem arising in the precise measurements of EF, we mention the calibration of the energy scale for electrons that is set by the potential difference between the cathode and the accelerating anode. Errors in the determination of a true energy of electrons depend on the error in the determination of contact potential difference, the

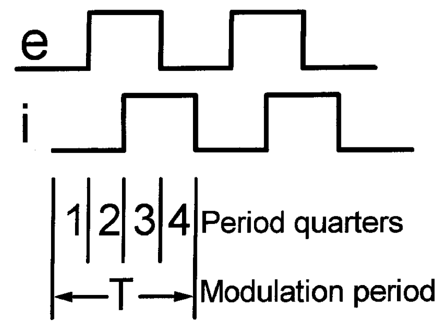

Fig. 2. Scheme of modulation of the electron and ion beams

decelerating effect of the spatial charge of an electron beam on the energy of electrons that flew through the "cathode — controlling anodes of the electron gun" gap, and the accelerating action of the ion beam on the energy of electrons in the beam.

As was shown in works [7,8], a true energy of electrons is given in the general case by the following formula:

$$eU_{\text{true}} = e\left(U_{\text{acc}} - U_K - \frac{S_e I_e}{U_{\text{true}}^{1/2}} + \frac{S_i A_i^{1/2} I_i}{U_i^{1/2}}\right), \qquad (2)$$

where eU_{true} — true energy of electrons, U_i and U_{acc} — accelerating voltages for ions and electrons, U_c — contact potential difference, S_e and S_i — geometric constants depending on parameters of the beams, I_e and I_i — total electron and ion currents, and A_i — atomic weight of an ion. The geometric constants S_e and S_i have dimensionality $[B^{3/2}\ /\mu\text{A}]$ and are determined experimentally for every setup.

For the estimation of the energy spread of electrons in a beam, work [8] presents the formula taking into account the effect of a spatial charge:

$$e\Delta U_e = e\left(\Delta U_{\text{t}} + \frac{S_e I_e}{U_{\text{true}}^{1/2}}\right), \qquad (3)$$

where $e\Delta U_{\text{t}}$ — thermal spread of the electron energy equal to $e\Delta U_{\text{t}} \approx 0.22$ eV for oxide cathodes, S_e– geometric constant with dimensionality $[B^{3/2}\ /\ \mu\text{A}]$, eU_{true} — true electron energy, and I_e — total electron current.

It is seen from (2) that the true electron energy depends on the total currents of electrons I_e and ions I_i that are used in the experiment and are functions of U_{acc} for U_i =const and A_i =const. As seen from (3), the energy spread of electrons in a beam depends on the total current of electrons I_e and is a function of the true energy eU_{true}.

The automation of the experiment with the use of a personal computer and CAMAC modules enabled us to directly experimentally determine the contact potential difference equal to ∼1.8 eV, and the decelerating voltage defined by the spatial charge of the electron beam, ∼0.3 eV, and the accelerating voltage due to the ion beam, ∼0.4 eV. With regard for these factors, the calibration of the energy electron scale was performed to within ±0.05 eV both for the ascending section of the voltage-current characteristic of the electron gun and beyond the threshold section of EF of the resonance line $\lambda = 228.8$ nm of Cd atoms, for which the spectroscopic excitation threshold is well known.

While studying the excitation of ions by electrons, the procedure of measurements was carried out, as a rule, in three stages. On the first one, we studied the electron excitation spectra of ions with the purpose to elucidate the position of the spectral lines under study and to preliminarily estimate the ratio of their intensities.

On the second stage, we measured the optical EF, $f(E)$, of spectral lines with wavelength λ, namely the relative intensities of these lines for various values of the electron energy:

$$f(E) = C/I_e, \quad (4)$$

where C is the valid signal and I_e is the total electron current.

The measurement of EF was performed by the scanning of the energy of electrons and the simultaneous measurement of the valid signal amplitude from the process under study at every specific energy during the identical time intervals. In this case, we considered that the measured EF is different from the true $f_{\text{true}}(E)$. This can be explained by the following circumstance. Since electrons of the beam have a certain real energy distribution $g(E)$, the measured EF $f_{\text{exp}}(E)$ is, in fact, a convolution of two functions $g(E)$ and $f_{\text{true}}(E)$. The application of electron beams with high monoenergeticity decreases the difference between $f_{\text{exp}}(E)$ and $f_{\text{true}}(E)$ and allows one to study such fine effects in EF as resonances. But various methods of monochromatization considerably decrease the electron current and, therefore, are used only in studying the most intense spectral transitions. The most optimum values of the energy homogeneity of electrons, for which one can else reliably study the structural peculiarities on EF in the precise measurements of electron-ion collisions, are $\Delta E_{1/2} = 0.2 \div 0.4$ eV on a half-height of the distribution curve.

On the third stage, we determined absolute values of the effective excitation cross-sections. To determine absolute values of the excitation cross sections for DS of the resonance lines of Cd^+ ions, we chose the energy interval for electrons so that to measure, in one experiment, DS and the threshold sections of EF of the resonance lines, for which absolute values of the effective cross sections were derived by us earlier [9] by normalization of the measured EF at an energy of 40 eV on the theoretical R-matrix-based calculation within the strong-coupling method for 15 states [10].

The valid signal was accumulated cyclically at each point with the exposure time of 10÷30 s and the number of cycles of 100—200. In this case, the dispersion of the accumulated number of valid pulses at the maximum of EF did not exceeded 10% for the resonance lines of Cd^+ ions and 30% for the DS of these lines.

2. Results of the Study and Discussion

In the course of the performed experiments, we observed the emission on the wavelengths of two resonance lines ($\lambda = 226.5$ and 214.4 nm, respectively), which appears only in the presence of Cd^+ ions in the chamber of collisions at the energies of electrons, being less than the excitation thresholds of the resonance levels of Cd^+ ion (5.47 eV for the $5p^2P^0_{1/2}$ level and 5.78 eV for the $5p^2P^0_{3/2}$ level). In order to ensure a clear separation of components of the resonance doublet of Cd^+ ion and to obtain, in this case, the maximum transmission of satellite lines, we carried out the studies in the intervals of wavelengths 224.5÷228.5 and 212.4÷216.4 nm. The results of studies of EF on near-threshold sections of the resonance lines of Cd^+ ion and of their DS in the energy interval 3.5 ÷6.5 eV are given in Figs. 3 and 4. At experimental points, the vertical bars show the mean square errors of relative measurements. Absolute values of the effective cross sections are derived with errors of at most 15%.

As seen from Figs. 3 and 4, the studied energy dependences reveal the well-pronounced structure prior to the excitation thresholds of the resonance levels of Cd^+ ion and above them. Maxima of the structure have the half-height width equal to the monoenergeticity of the electron beam, i.e., they have a resonance character. This fact suggests the idea of that they are defined by the resonant capture of incident electrons by Cd^+ ions with excitation of the "electron + ion" system into AIS of Cd atom of the $4d^{10}5p(^2P^0_{1/2,3/2})ns, (n-1)d$ and $4d^9(^2D_{5/2,3/2})5s^2np, (n-1)f$ configurations (where $n \geq 5$) and with their following decay through the electron and radiative channels. If the electron decay

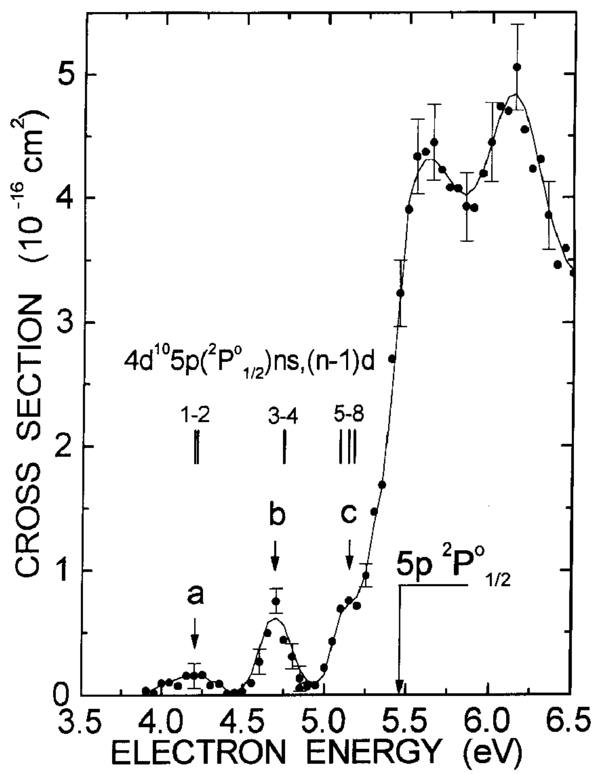

Fig. 3. Effective cross section of excitation of the resonance line $\lambda = 226.5$ nm of Cd^+ ions and its dielectronic satellites (peculiarities *a*, *b*, and *c*) versus energy

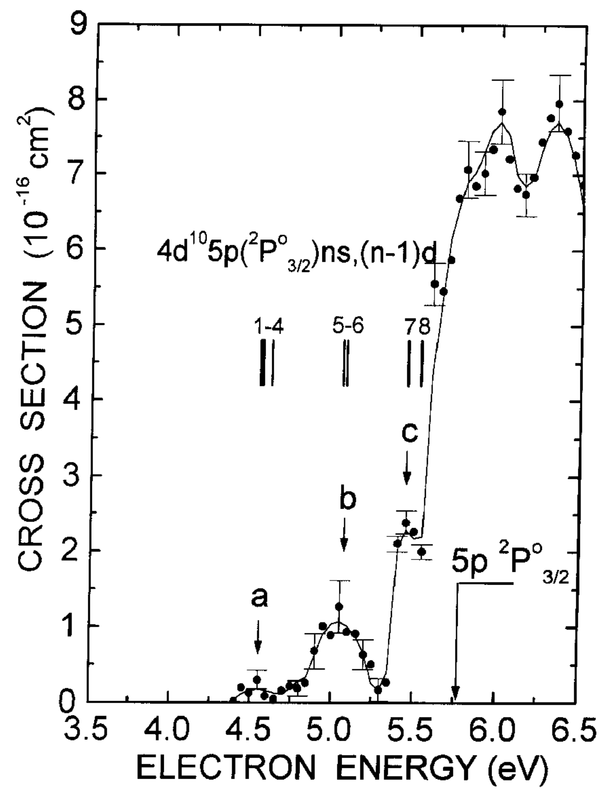

Fig. 4. Effective cross section of excitation of the resonance line $\lambda = 214.4$ nm of ions Cd^+ and its dielectronic satellites (peculiarities *a*, *b*, and *c*) versus energy

of such AIS leads to a resonance structure above the excitation thresholds for resonance levels, then the subthreshold structure is related to the radiative stabilization of the $4d^{10}5p(^2P^0_{1/2,3/2})ns, (n-1)d$ AIS of Cd atom into the excited $4d^{10}5sns, (n-1)d^{1,3}L_j$ levels of Cd atom in the process of DR, i.e., the observed emission is DS of resonance lines.

The analysis of the derived results with regard for the data on the energy positions and configurations of AIS of Cd atoms [11—12] (see the table) showed that the separate maxima (a) in the energy dependences at an energy of 4.25 eV in Fig. 3 and at 4.60 eV in Fig. 4 are most probably related to the decay of the $4d^{10}5p7s$ AIS, and the effective maxima (b) at energies of 4.70 eV in Fig. 3 and 5.1 eV in Fig. 4 are related to the decay of the $4d^{10}5p8s$ AIS into the $4d^{10}5snl\ ^{1,3}L$ levels of an atom of Cd ($n = 7$ and 8). Beginning from n $\geq$9, AIS of the $4d^{10}5p(^2P^0_{1/2,3/2})ns, (n-1)d$ configurations are very densely positioned in a narrow energy interval. Therefore, DS are not separated spectroscopically and give a summary contribution to the process of DR [see, e.g., peculiarities (c) on EF at energies of 5.21 eV in Fig. 3 and 5.5 eV in Fig. 4]. However, as seen from the table, the energies of maxima (c) most probably coincide in this case also with the energies of the $4d^{10}5p10s$ and $4d^{10}5p11s$ AIS. This yields that the greatest contribution to the emission of DS is given by AIS of the $4d^{10}5p(^2P^0)ns$ configuration. It is worth noting the following regularity: DS of the resonance line $\lambda = 226.5$ nm ($5^2P^0_{1/2} \rightarrow 5^2S_{1/2}$) are the spectral lines emitted under the decay of AIS, for which the convergence limit is the $5p^2P^0_{1/2}$ level. For the resonance line $\lambda = 214.4$ nm ($5^2P^0_{3/2} \rightarrow 5^2S_{1/2}$), spectral lines converge to the $5p^2P^0_{3/2}$ level. However, the theoretical calculations performed in [12] with the use of the HXR program [13] showed that the energy region contained, besides DS discovered by us, AIS with a strong configuration mixing of levels (see the table). In our opinion, this fact is one of the important factors to increase the probability of their radiative decay.

At energies close to the excitation thresholds of the resonance levels (5.47 and 5.78 eV), we failed to separate the energy dependences of the effective cross sections of DS and those for the excitation of resonance lines. The reason for this is the energy electron spread. However, it is seen that the ascending sections of EF of both components of the resonance doublet contain a number of peculiarities in the form of bends coinciding by energy with AIS of Cd atom. This indicates that the radiative decay of AIS close by energy to the excitation thresholds of resonance levels influences considerably the resonance excitation, by decreasing its effective cross section. Beginning from the energies of the excitation thresholds of resonance levels, we observed the efficient excitation of AIS of the $4d^9(^2D_{5/2,3/2}5s^2np,(n-1)f$ configurations which made a considerable (~20—30%) resonant contribution to the effective excitation cross sections of both the resonance lines.

Conclusion

We have first studied the energy dependence of the effective excitation cross-sections for DS of the resonance lines of Cd^+ ion and have shown that absolute values of the cross sections of their excitation are $(0.2\div1)\cdot10^{-16}$ cm^2, i.e., they are of the same order as the effective cross sections of excitation of the resonance lines of this ion [9]. At the same time, we note that ions Mg^+ and Ca^+, which belong also to the II group of the Periodic system of elements, have the structure of the external electron shell (one s-electron) similar to that of Cd^+ ions, but differ from the latter by the subvalent shell (their subvalent shell is the p^6-shell), possess the effective excitation cross-sections of DS to be 10^{-17} cm^2 by the order of magnitude [14, 15], i.e., they are less almost by two orders than the effective excitation cross-sections of the relevant resonance lines [16].

We have shown that the main mechanism of excitation of the satellites of resonance lines of Cd^+ ions is DR. Moreover, the direct process of excitation of the ions influences DR only mediately, through its influence on the probability of autoionization. However, the resonance excitation strongly influences DR, because these two channels are related to competitive processes. On the contrary, our investigations showed that, at the excitation thresholds of resonance levels, DR leads to a decrease in the resonance excitation efficiency.

The efficiency of DR significantly depends on the ratio of the probabilities of the radiative and electron decays of AIS. For a relativistic Cd^+ ion, a strong configurational mixing of levels occurs, which causes the considerable increase in the probability of the radiative decay of AIS.

Identification of the studied maxima of the DS of resonance lines of Cd^+ ions

Maximum on EF: λ, nm		Energy of a maximum, eV	N of AIS	Energy of AIS, eV [sourse]	Configuration of AIS
226.5±2.0	*a*	4.20	1	4.193 [12]*	$4d^{10}5p(45\%5d\,^1P_1+24\%7s\,^1P_1+20\%7s\,^3P_1)$
			2	4.21 [11]	$4d^{10}5p(^2P^0_{1/2})7s^3P_1$
			2	4.22 [12]*	$4d^{10}5p(99.7\%7s^3P_1)$
	b	4.70	3	4.740 [12]*	$99.6\%\ 8s\,^3P_1$
			4	4.743 [11]	$4d^{10}5p(^2P^0_{1/2})8s$ [1/2]
			4	4.744 [12]*	$67\%8s^3P_1+31\%8s^1P_1$
	c	5.15	5	5.08 [12]*	$4d^{10}5p(51\%8s\,^1P_1+20\%8s^3P_1+11\%7d\,^3D)$
			5	5.09 [11]	$4d^{10}5p(^2P^0_{1/2})8d$
			6	5.14 [11]	$4d^{10}5p(^2P^o_{1/2})10s$
			7	5.176 [12]*	$4d^{10}5p(59\%7d^1D+20\%7d^3F+15\%7d^3D)$
			8	5.177 [12]*	$99\%7d\,^3F$
214.4±2.0	*a*	4.60	1	4.54 [11]	$4d^{10}5p(^2P^0_{3/2})7s\,^1P_1$
			2	4.55 [12]*	$4d^{10}5p(37\%7s\,^3P+23\%6d\,^3D+23\%6d\,^3P+14\%6d\,^1D)$
			3	4.56 [12]*	$4d^{10}5p(60\%6d\,^3F+22\%6d\,^3D+13\%6d\,^1F)$
			4	4.61 [12]*	$4d^{10}5p(49\%6d\,^3D+22\%7s\,^1P+11\%6d\,^3P)$
	b	5.10	5	5.05 [12]*	$99\%4d^{10}5p8s\,^3P$
			5	5.06 [11]	$4d^{10}5p(^2P^o_{3/2})8s$
			6	5.08 [12]*	$4d^{10}5p(51\%8s^1P+20\%8s\,^3P+11\%7d\,^3D)$
	c	5.50	7	5.45 [11]	$4d^{10}5p(^2P^0_{3/2})10s\ [3/2]_1$
			8	5.53 [11]	$4d^{10}5p(^2P^o_{3/2})11s\ [3/2]_1$

*Calculations by the HXR program [13].

1. *Massey H.S.W., Bates D.R.* // Repts. Prog. Phys. — 1942. — **9**. — P.62—69.
2. *Burgess A.* // Astrophys. J. — 1964. — **139**. — P.776—779.
3. *Vainshtein L.A., Sobel'man I.I., Yukov E.A.* Excitation of Atoms and Broadening of Spectral Lines. — Moscow: Nauka, 1979 (in Russian).
4. *Gomonai A.N., Imre A.I., Kontrosh E.E.* // Opt. Spektr. — 1996. —**81**, N1. — P.29—32.
5. *Imre A.I., Gomonai A.N., Vukstich V.S., Nemeth A.N.* // Pis'ma ZhETF. — 1998. — **68**, Iss. 8. — P.614—617.
6. *Gomonai A.N. Imre A.I., Vukstich V.S., Nemeth A.N.* //Contributed Papers XXI Intern. Conf. on Physics of Electronic and Atomic Collisions (XXI ICPEAC), Sendai, Japan, July 22—27, 1999.— P.342.
7. *Taylor P.O., Dunn G.H.*// Phys. Rev. A. — 1973. — **8**. — P.2304—2321.
8. *Rogers W.T., Olsen J.O., Dunn G.H.* // Ibid. — 1978. — **18**, N4. — P.1353—1362.
9. *Gomonai A.N.* // Opt. Spektr. — 2003. — **94**, Iss.4. —P.714—721.
10. *Zatsarinnyi O.I., Bandurina L.A.* // Ibid. — 2000. — **89**, Iss.4. — P.546—554.
11. *Mansfield M.W.* // Proc.Roy.Soc. (London) A. — 1978. — **362**. — P.129—144.
12. *Mansfield M.W., Murnane M.M.* // J. Phys. B: Atom and Mol. Phys. — 1985. — **18**. — P.4223—4244.
13. *Cowan R.D., Griffin D.C.* // J. Opt. Soc. Amer. —1976. — **66**. — P.1010—1014.
14. *Belic S., Dunn G.H., Morgan T.J. et al.* // Phys. Rev. Lett. — 1983. — **50**. — P.339—343.
15. *Williams J.F.* // Phys. Rev. A. — 1984. — **29**, N5. — P.2936—2938.
16. *Zapesochnyi I.P., Imre A.I., Dashchenko A.I., Frontov V.I.* // Zh. Eksp. Teor. Fiz. — 1991. — **100**, Iss.1(7). — P.113—124.

Received 03.03.03
Translated from Ukrainian by V. V. Kukhtin

ЗБУДЖЕННЯ ДІЕЛЕКТРОННИХ САТЕЛІТІВ РЕЗОНАНСНИХ ЛІНІЙ ІОНА КАДМІЮ ПРИ ЕЛЕКТРОН-ІОННИХ ЗІТКНЕННЯХ

Г.М Гомонай, А.Й. Імре

Р е з ю м е

Запропоновано ідентифікацію виявлених допорогових особливостей на експериментально досліджених енергетичних залежностях ефективних перерізів електронного збудження резонансних ліній $\lambda = 226,5$ та 214,4 нм іона Cd^+. Експеримент виконано спектроскопічним методом в умовах пучків моноенергетичних електронів й іонів, що перетинаються під кутом 90°. Встановлено, що допорогові особливості є результатом резонасного захоплення налітаючого електрона іоном, збудження системи "електрон + іон Cd^+" в автоіонізаційні стани $4d^{10}5p(^2P_{1/2,3/2})nl$ та їх радіаційного розпаду на збуджені $4d^{10}5snl$-стани атома Cd, тобто є діелектронними сателітами резонансних ліній. Абсолютні величини перерізів збудження діелектронних сателітів дорівнюють $(0.2\div1)\cdot10^{-16}$ см^2 і є величинами одного порядку з ефективними перерізами збудження резонансних ліній іона Cd^+. Показано, що суттєве зростання ймовірності радіаційного розпаду автоіонізаційних станів $4d^{10}5p(^2P_{1/2,3/2})nl$ атома Cd пов'язане з сильним конфігураційним змішуванням синглетних і триплетних рівнів цих станів.